Small-angle scattering and the structure of ambient liquid water

Gary N. I. Clark[a], Greg L. Hura[b], Jose Teixeira[c], Alan K. Soper[d], and Teresa Head-Gordon[a,b,1]

[a]Department of Bioengineering, University of California, Berkeley, CA 94720; [b]Physical Biosciences Division, Lawrence Berkeley National Laboratory, Berkeley, CA 94720; [c]Laboratoire Leon Brillouin Commissariat à l'énergie atomique et aux énergies alternatives/Centre National de la Recherche Scientifique (CEA/CNRS), CEA Saclay, 91191 Gif-sur-Yvette Cedex, France; and [d]Integrated Standby Instrument System (ISIS) Facility, Science and Technology Facilities Council (STFC) Rutherford Appleton Laboratory, Harwell Science and Innovation Campus, Didcot, Oxon, OX11 0QX, United Kingdom

Structural polyamorphism has been promoted as a means for understanding the anomalous thermodynamics and dynamics of water in the experimentally inaccessible supercooled region. In the metastable liquid region, theory has hypothesized the existence of a liquid-liquid critical point from which a dividing line separates two water species of high and low density. A recent small-angle X-ray scattering study has claimed that the two structural species postulated in the supercooled state are seen to exist in bulk water at ambient conditions. We analyze new small-angle X-ray scattering data on ambient liquid water taken at third generation synchrotron sources, and large 32,000 water molecule simulations using the TIP4P-Ew model of water, to show that the small-angle region measures standard number density fluctuations consistent with water's isothermal compressibility temperature trends. Our study shows that there is no support or need for heterogeneities in water structure at room temperature to explain the small-angle scattering data, as it is consistent with a unimodal density of the tetrahedral liquid at ambient conditions.

anomalous scattering | density distribution | isothermal compressibility | structural polyamorphism

Water appears to be a unique liquid relative to other fluids in exhibiting several anomalous features of structure, thermodynamics, and dynamics. Both experiment and molecular dynamics simulation have shown that water in the metastable supercooled region exhibits response functions and transport properties that appear to diverge near −45 °C (1). Below its glass transition temperature, experimental evidence shows that there are polyamorphic states of water, in particular the formation of low-density amorphous and high-density amorphous glasses (2, 3). This polyamorphism has been promoted as a means for understanding the anomalous thermodynamics and dynamics of water, such as the large increase in its isothermal compressibility with decreasing temperature, when extrapolated into the experimentally inaccessible supercooled liquid region (3, 4). Polyamorphism underlies one of the main assumptions of the second critical point hypothesis (5), i.e., the postulated existence of a liquid-liquid critical point from which a dividing line separates two fluctuating species of high and low-density liquids (HDL and LDL).

However, recent studies have shown that while there may be low-temperature criticality in the ST2 water model, there is no need to invoke an explanation for a second critical point in water based on structural polyamorphism (6). Furthermore, it is also possible to explain the existing anomalies without invoking an additional thermodynamic singularity, in the so-called singularity-free interpretation (4, 7). Sastry and coworkers have shown that a finite increase in isothermal compressibility upon lowering the temperature of a liquid that expands upon cooling (like water) is a thermodynamic necessity, and was illustrated for a water-like lattice model that has no singularities (7). This diversity in possible explanations for the thermodynamic and kinetic anomalies emanating from the supercooled state of water is a highly engaging but unresolved problem in liquid state physics.

At temperatures far above the hypothetical critical point, ambient water (like any material above a critical region) would be expected to exhibit a single homogeneous phase. Since the late 1970's it has been accepted that the structure of bulk liquid water under ambient conditions is, on average, uniformly tetrahedral (8–10). Although thermal fluctuations give rise to distortions from idealized hydrogen-bond geometries depending on the instantaneous local environment, integration under the first peak of the oxygen-oxygen radial distribution function, $g_{OO}(r)$, at room temperature gives an estimate of the nearest neighbor coordination number somewhere between 4 and 5, indicating that water preserves much of its ice-like tetrahedral structure (11–13). This general structural picture of water as a tetrahedral liquid has helped contribute to our greater understanding of a broad range of experiments including the dynamics and thermodynamics of the liquid state (8, 10, 14, 15).

Recently, Huang et al. (16) used small-angle X-ray scattering (SAXS) over the temperature range 7–77 °C, to show the existence of a shallow minimum in the structure factor, $S(Q)$, at small but finite Q which then rises to the $S(Q = 0)$ value consistent with water's isothermal compressibility at a given temperature. They attribute the minimum in SAXS intensities as being connected with a difference in density between two structural species, which they analyze with a Guinier treatment usually reserved for determining the shape and size of macromolecules in a multicomponent solution. Furthermore, they use the SPC/E model (17) to show that a tetrahedral model of water lacks such structural signatures in the same small-Q region, concluding that representation of water as a (distorted) tetrahedral network are inconsistent with the new SAXS data. Instead, Huang et al. use previously reported X-ray absorption, Raman and Emission spectroscopy (XAS, XRS and XES) data (16, 18), which are in themselves controversial (10), to describe the two distinct water structural species as the hypothetical LDL and HDL polyamorphs postulated to be present in the supercooled region, which they argue persist and are observable at ambient temperatures.

In this work we present both new SAXS data on liquid water taken at the Advanced Light Source (ALS) as well as molecular dynamics simulations of 32,000 water molecules using the TIP4P-Ew model (19), to access the correlation lengths of fluctuations present in $S(Q)$ down to $Q \sim 0.03$ Å^{-1} and $Q \sim 0.14$ Å^{-1}, respectively. We show that the measurements from any of the available SAXS experiments conducted at ambient temperatures are simply interpreted as number fluctuations that arise from stochastic processes for a single component fluid (20). In particular, we

CHEMISTRY

show that Huang et al. have misrepresented standard density fluctuations as "concentration fluctuations" to justify a shape and size of ~13–14 Å for their iceberg-like LDL polymorphic structure. Furthermore, we show that the TIP4P-Ew model reproduces the same $S(Q)$ features as the SAXS experiments at ambient conditions, without giving any indication of structural heterogeneities in its density distributions. We conclude that modern simulation models of water and SAXS experiments on liquid water cannot support the existence of polymorphism at room temperature, and instead reaffirm that ambient water is a homogeneous tetrahedrally coordinated liquid.

Results

Fig. 1 compares the SAXS room temperature data from Bosio et al. 1981 (21), with Huang et al., 2009 (16), and our new ALS 2009 data, in the range of momentum transfer, Q, of $0.03 \text{ Å}^{-1} \leq Q \leq 0.8 \text{ Å}^{-1}$. Like Huang et al. (16) we place the ALS 2009 data on an absolute scale by enforcing the 25 °C data to extrapolate to the isothermal compressibility limit as derived from thermodynamic fluctuation and kinetic theory (22)

$$S(0) = k_B T \rho_N \chi_T, \qquad [1]$$

where k_B is Boltzmann's constant, T is the temperature, ρ_N is the molecule number density, and χ_T is the isothermal compressibility reported in ref. 23. There are some differences in the structure factor data between experiments, although the scale in Fig. 1 is rather unforgiving (exhibited over a fraction of electron units (e.u.)) so that all datasets are in quantitative disagreement at this scale. Overall the experimental design reported by Huang et al (16) is virtually identical to the ALS experiment, except for one important difference. Our ALS experiment used only one detector position to capture our 0.03–0.3 Å^{-1} data range, while Huang et al used three different detector positions to capture their 0.04–0.8 Å^{-1} range, requiring them to piece together three different datasets to create a single curve. However no information is given in their paper as to how the datasets were matched to render the single curve shown in Fig. 1, or whether each data window required different corrections (as would be expected). For all temperatures considered a minimum in $S(Q)$ is clearly visible, in agreement with the experimental data of Bosio 1981 and Huang 2009 that go out to wider angle than the ALS 2009 study. The shallow minimum in $S(Q)$ was attributed by Huang et al to be an experimental signature of a bimodal water density in which
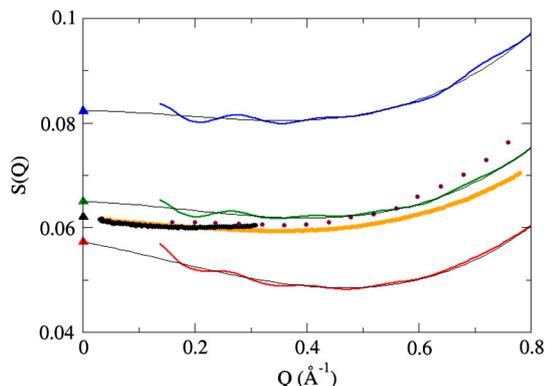
there are "low-density" patches of ~13–14 A in a sea of dissociated higher density liquid (16).

To complement our SAXS experimental study we present analysis of the small-Q-region for the TIP4P-Ew model of water (19), also shown in Fig. 1, which shows the calculated structure factor data in the range $0.14 \text{ Å}^{-1} \leq Q \leq 1.0 \text{ Å}^{-1}$ for −37.5 °C, 25 °C, and 75 °C. Fig. 2 shows that the artificial oscillations in $S(Q)$ are the result of Fourier truncation errors, but these have been better suppressed by evaluating the radial distribution functions (RDFs) in the grand canonical ensemble, as opposed to evaluating the RDFs in a fixed volume (NVT) ensemble as was done in refs. 16, 24. Because the TIP4P-Ew model shows the same $S(Q)$ signature of a minimum and then rise at small-angle, we show its density distribution when evaluated over different length scales in Fig. 3; it is evident that regardless of length scale analyzed, the density is always unimodal.

For a homogeneous single component liquid far from any critical region, the small-Q region of the scattering profile of a homogeneous fluid measures the length scale, l_N, over which number fluctuations

$$\lim_{Q \to 0} S(Q) = \frac{\langle (N - \langle N \rangle)^2 \rangle}{\langle N \rangle} \qquad [2]$$

are still observable in Q-space (20, 25). To determine evidence of enhanced or anomalous density fluctuations, such as that found near a critical point, one can then separate the total intensity or structure factor into normal $S^N(Q)$ and anomalous $S^A(Q)$ components (26)

$$S(Q) = S^N(Q) + S^A(Q). \qquad [3]$$

The decomposition of a property into normal and anomalous components is justified whenever "cooperative" behavior is observed and anomalous fluctuations are found to be superimposed on the "normal" fluctuations characteristic of the property in question (1).

The normal component of scattering is either assumed to be Q-independent, i.e., $S^N(Q) = S^N(0)$ over the small-Q region (21, 27), where

$$S^N(0) = k_B T \rho_N \chi_T^N \qquad [4]$$

and χ_T^N is the normal component of the isothermal compressibility, or is extrapolated with Q-dependence from $S(Q)$ at larger values of Q under the constraint of reaching the $S^N(0)$ limit as was done in ref. 16. In the latter case it is assumed there is no anomalous $S^A(Q)$ contribution to $S(Q)$ at larger values of Q, although the Q range over which this assumption is made appears

Fig. 1. Small-angle X-ray scattering experiments and TIP4P-Ew simulation. Comparison of the structure factor, $S(Q)$, for the experimental ALS 2009 (*black* spheres), Huang 2009 (16) (*orange* spheres) and Bosio 1981(21) (*maroon* spheres) data at 25 °C, and the calculated TIP4P-Ew data at 75 °C (*blue* line), 25 °C (*green* line), and −37.5 °C (*red* line). The triangles at $Q = 0$ are the result of calculation based on thermodynamic properties in Eq. 1 reported by Horn et al. with the black triangle corresponding to experiment at 25 °C. A polynomial fit over the range $0.13 \text{ Å}^{-1} \leq Q \leq 1.0 \text{ Å}^{-1}$ constrained to $S(0)$ is shown for each simulated temperature (—).
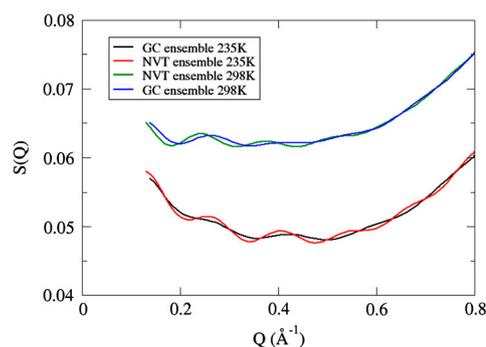

Fig. 2. Simulated small-angle structure factor calculated in the grand canonical vs. canonical ensembles. Comparison of the calculated $S(Q)$ for the TIP4P-Ew model calculated at −37.5 °C in the grand canonical ensemble (*black* line) and canonical ensemble (*red* line) and at 25 °C in the grand canonical ensemble (*blue* line) and canonical ensemble (*green* line). Both ensembles were evaluated with the same number of statistics.
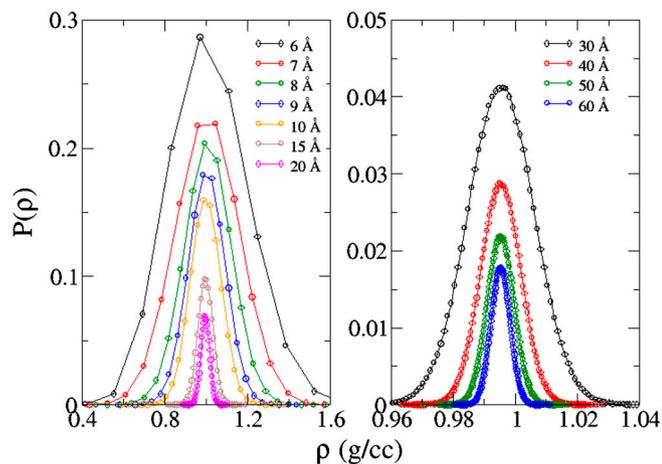
Fig. 3. Density distribution of TIP4P-Ew evaluated at different length scales. The density probability calculated over randomly sampled boxes of different lengths.

to be arbitrary in practice (16, 21, 28). The point is that there is no clearly defined way to determine $S^N(Q)$.

Once an estimate of the normal component is subtracted from the total structure factor, the anomalous component allows for the calculation of the Ornstein-Zernike (O-Z) correlation length ξ, by fitting it to the following Lorentzian functional form

$$S^A(Q) = \frac{A(T)}{\xi^{-2} + Q^2}, \qquad [5]$$

where $A(T)$ is a temperature specific constant (26). For a homogeneous liquid, the correlation length derived from the O-Z analysis of small-angle scattering data is interpreted to be the size of an observation window in which density fluctuations are still observable in inverse space, but is only valid when $Q \rightarrow 0$ and $S(0) \gg 1$. It is important to emphasize that far from a critical point, such as that near room temperature, the anomalous component will necessarily be small relative to the normal component, and difficult to determine with any confidence.

Table 1 shows correlations lengths calculated under the assumptions (1) $S^N(Q) = S^N(0)$ and (2) $S^N(Q)$ is extrapolated with Q-dependence from $S(Q)$ at larger values of Q (see *Methods*). Under assumption (1), the correlation lengths determined from the Huang 2009 and ALS 2009 SAXS data are small and in close agreement, 1.25 Å and 1.2 Å, respectively; this serves to highlight that both of these independently obtained datasets are virtually identical over the same Q-range and under this version of the O-Z analysis. The calculation of $S^A(Q)$ under assumption (2) leads to a slightly larger value of the correlation length for the Huang 2009 data (3.1 Å). Using the same O-Z analysis on the TIP4P-Ew model at room temperature we determine correlation lengths of 1.3 Å and 2.8 Å under assumption (1) and (2) respectively (Table 1), and is within the range of the experimental results.

Fig. 4 shows the corresponding Lorentzian fits to $S^A(Q)$ over the Q-range of 0.03–0.04 Å^{-1} ≤ Q ≤ 0.2 Å^{-1} using the two ways

to estimate $S^N(Q)$. It is seen that the Lorentzian fits to the anomalous component can not conform well to both the $S^A(Q)$ data and the $S^A(0)$ limit for any of the experimental datasets. The poor fit combined with the fact that the correlation lengths are small emphasizes the point that the anomalous component is negligible under ambient conditions, showing that the O-Z analysis is invalid far away from a critical point and should not be applied to SAXS water data at room temperature. We conclude that the ambient water liquid is dominated by normal fluctuations and that the correlation lengths are indeterminately small.

Discussion

One of the earliest experimental investigations of water in the small-Q region was by Hendricks et al. (1974) (29) who used X-ray scattering to estimate the structure factor $S(0)$ over the temperature range 6 °C < T < 75 °C. Using experimental values of the isothermal compressibility χ_T (23), Hendricks et al. found good agreement between their experimentally estimated values of $S(0)$ and those calculated using Eq. **1**, with a minimum in $S(0)$ at ~20 °C that corresponds to the minimum in the isothermal compressibility at ~46 °C. Subsequent small-angle liquid scattering experiments SAXS (21, 27, 30, 31) and small angle neutron scattering (SANS) (28, 32) on water have mainly been concerned with the existence of density fluctuations in the supercooled state, and their connection to the possible divergence of response functions such as the isothermal compressibility with decreasing temperature (4).

There is clear consensus over several decades that the O-Z correlation length is not larger than the molecular size, independent of the dataset analyzed. The first estimation of the length scale of density fluctuations in liquid water was by Bosio et al. (21) (1981) who used X-ray scattering to measure the structure factor $S(Q)$ of water in the range 0.15 Å^{-1} < Q < 1.0 Å^{-1} and −20 °C < T < 75 °C. Bosio et al. obtained a correlation length of ~8.0 Å for supercooled water at the lowest temperature considered, which was revised down to ~6.0 Å in a later SANS study (28). A later SAXS experiment by Xie et al., 1993 (27) investigated density fluctuations in the range 0.05 Å^{-1} < Q < 0.30 Å^{-1} and −34 °C < T < 25 °C, and determined correlation lengths that remained constant with temperature, between ~2.0–3.8 Å depending on how the normal component of scattering is estimated, consistent with values reported by Dings and coworkers (31). Consistent with these data in the lightly supercooled regime, the TIP4P-Ew model at −37.5 °C estimates correlation lengths of 3.0 Å and 2.1 Å depending on how the normal component is determined (Table 1). Based on Lorentzian fits to the very small $S^A(Q)$ measured near ambient conditions, Huang et al. calculate correlation lengths of the liquid to be ~3.1 Å, which remain flat with temperature, consistent with all previous studies.

Nevertheless, the applicability of the O-Z analysis appears questionable. It is clear that regardless of the assumption employed to calculate the normal contribution to $S(Q)$ the correlation length remains small, such that the choice of method employed is qualitatively unimportant. The use of the O-Z relation in Eq. **5**, which is based on a Taylor expansion of $S(Q)$ for small Q, is only valid when $S(0) \gg 1$, i.e., that expected near a

Table 1. The Ornstein-Zernike correlation lengths ξ of water as a function of temperature

Temperature (°C)	Correlation length ξ (Å)				
	ALS 2009 (2)	Huang 2009 (1)	Huang 2009 (2)	TIP4P-Ew (1)	TIP4P-Ew (2)
75–80	—	2.8 (3.0)	1.45	2.7	1.1
25	1.2	3.1 (3.1)	1.25	2.8	1.3
−37.5	—	—	—	3.0	2.1

Derived from the SAXS experiments reported here (ALS 2009) and from Huang et al. 2009 (16), and from simulated TIP4P-Ew data. The correlation lengths are estimated from two procedures for evaluating the normal component of scattering: (1) $S^N(Q)$ dependent on Q and (2) $S^N(Q) = S^N(0)$ (see *Methods*). The numbers in parentheses are values reported in ref. 16.
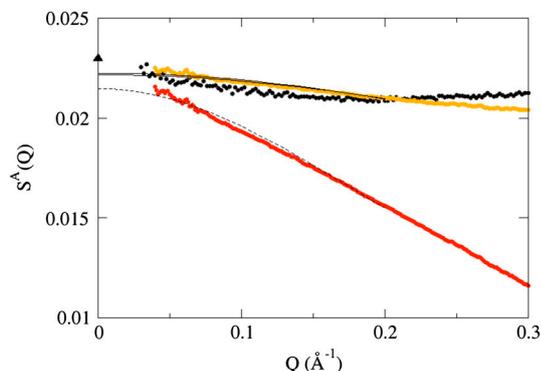
Fig. 4. Ornstein-Zernike analysis of experimental SAXS data. A comparison of the Lorentzian fits calculated using $S^N(Q)$ dependent on Q (—) and S^N constant over the Q-range (—) to the experimental ALS 2009 (*black*) and Huang 2009 (16) (*orange* and *red*) anomalous structure factor component $S^A(Q)$ data at 25 °C. The triangle is the estimated anomalous scattering at $S^A(0)$.

critical point. The correlation length ξ becomes equivalent to l_N only when fluctuations diverge near a critical point—and since room temperature water is in the single phase region well above the supercooled region—the small-angle region should be analyzed from the perspective of Eq. **2** even if that second critical point were to exist.

Finally we comment on mixture models, namely that distinct thermodynamically stable molecular species exist in the ambient liquid, used by Huang et al. to analyze their SAXS data. Finally we comment on mixture models, namely that distinct thermodynamically stable molecular species exist in the ambient liquid. Huang et al. analyze their SAXS data using a mixture model when they relate the O-Z correlation length to a form factor to characterize a radius of gyration $R_g = 3^{1/2}\xi$ or diameter $D_s = 2(5/3)^{1/2}R_g \sim 13$–14 Å, which they associate with a LDL-like structural species of a bimodal density LDL-HDL mixture (16). The assumption of a mixture model implies that water at its compressibility limit is composed of both number fluctuations and concentration fluctuations, although there is absolutely no evidence in or theory of the low angle scattering data that compels one to adopt the assumption of bimodality in the density. Furthermore a bimodal density distribution in water should only exist in a two phase coexistence region *below* a second critical point (if it were to exist), and it necessarily becomes unimodal as soon as you enter the single phase region at higher temperatures.(33)

Huang et al. attribute the failure of the SPC/E model to exhibit these small-angle features over the same range of temperatures to a simulation model of water that is "too tetrahedral" to reproduce the "concentration fluctuations" observed in the SAXS experiment. It is well appreciated that a model such as ST2 (34) is too tetrahedral while models like SPC/E (17) are understructured.(35) In fact the minimum in isothermal compressibility and temperature of maximum density for SPC/E is at a temperature ~50 °C below that of experiment (36). It would be logical to conclude that the SPC/E model is incapable of getting sensible values of $S(0)$ and reproducing SAXS data at room temperature, and hence that failure would likely be because it is *not tetrahedral enough*. Paschek and coworkers have recently characterized the phase diagram of TIP4P-Ew, and found that the model "almost quantitatively matches the (experimental) compressibility and thermal expansivity of water up to pressures in the gigapascal range" (37). The TIP4P-Ew model also reproduces a minimum in $S(Q)$ and correlation lengths that are small which remain constant with temperature—consistent with the published small angle scattering (SAS) experiments on water taken at third generation synchrotron sources. When the density distribution

of the TIP4P-Ew model is analyzed over different lengthscales-it exhibits a unimodal density.

Conclusions

All small-angle scattering experiments on the ambient water liquid to date yield trends in $S(Q)$ that conform to the compressibility limit expected for a homogeneous liquid. The increase in $S(Q)$ at small angle is due to the normal density fluctuations which arise from stochastic processes in a single component fluid.(20, 25) The tetrahedral network forming TIP4P-Ew model of water qualitatively reproduces the trend in $S(Q)$ at ambient conditions and yields the same correlation lengths arrived at by experiment. An increase in $S(Q)$ at small angle is due to a play-off between attractive and repulsive intermolecular interactions that are completely consistent with a unimodal density. Regardless of the method employed to calculate the normal contribution to $S(Q)$ in an O-Z analysis, the correlation length remains small, consistent with an expected negligible anomalous component far above a hypothetical critical point. In summary, there is no evidence that supports the notion of structural polyamorphism in bulk water at ambient conditions, especially since the ambient water liquid should be homogeneous far above a critical point even if it existed in the supercooled region of real water.

Methods

SAXS experiments on water in the range $0.03 \text{ Å}^{-1} \leq Q \leq 0.3 \text{ Å}^{-1}$ at 25 °C were carried out at the SIBYLS beam line (beam line 12.3.1) (38) at the ALS at the Lawrence Berkeley National Laboratory. A beam energy of 12 keV was used and all water samples were deionized, degassed, and allowed to equilibrate for 2 min before exposure. Measurements were taken for both the water filled mica sample holder and the empty sample holder for short and long exposure times to check for radiation damage. No radiation damage was observed, and so the higher signal to noise measurement, with an exposure time of ~10.0 s, was used. Data collection and processing was conducted for 10 independent sets. All datasets were corrected for absorbance and scattering from the empty sample holder was subtracted. While our Q-range is more limited than the Huang et al. experiments, we did so to avoid the problem of having to match data over three different Q window experiments as was done in ref. 16.

The ALS intensity data at room temperature was placed on an absolute scale so that a polynomial fit extrapolation to $Q = 0$ over the region $0.05 \text{ Å}^{-1} \leq Q \leq 0.2 \text{ Å}^{-1}$ was consistent with the limit in the isothermal compressibility. The ALS intensity data at room temperature is placed on an absolute scale so that a polynomial fit extrapolation to $Q = 0$ over the region $0.05 \text{ Å}^{-1} \leq Q \leq 0.2 \text{ Å}^{-1}$ is consistent with the limit in the isothermal compressibility, as was also done in ref. 16. We transformed the experimental intensity, $I(Q)$, to structure factor data using

$$S(Q) = \frac{I(Q)}{\langle F(Q)^2 \rangle}, \qquad [6]$$

where the molecular form factor $\langle F(Q)^2 \rangle$ for water is that reported by Wang et al. (39).

We use the TIP4P-Ew model of water (19) to simulate trajectories in the NVT ensemble for the temperature range of $-37.5 \,°C \leq T \leq 75 \,°C$, in which system volumes were determined from the average densities evaluated in the isothermal-isobaric ensemble (and found to be consistent with that reported by Horn et al. (19)). Initial configurations of 32,000 water molecules were obtained using the PACKMOL software package (40). Using an in-house parallelized molecular dynamics code, the simulations were equilibrated for 0.3–1.3 ns and statistics collected over a further 0.5–1.5 ns depending on temperature.

The intensity spectra are calculated using

$$I(Q) = \langle F(Q)^2 \rangle + \sum_{i \leq j}(2 - \delta_{ij})x_i x_j f_i'(Q)f_j'(Q)S_{ij}(Q), \qquad [7]$$

where $\langle F(Q)^2 \rangle$ is the molecular form factor reported by Wang et al. (39), x and $f'(Q)$ are the atomic fractions and modified atomic scattering factors (MAFF's) (41) of atom types i and j, respectively, and $S_{ij}(Q)$ is the partial structure factor between atom types i and j.

$$S_{ij}(Q) = 4\pi\rho \int_0^\infty r^2 (g_{ij}(r) - 1) \frac{\sin Qr}{Qr} dr, \qquad [8]$$

where ρ is the atomic density, and $g_{ij}(r)$ is the radial distribution function describing intermolecular correlations between atom types i and j. The MAFF parameters correspond to a dipole moment of 2.8 Debye in the liquid phase and a shift of 2/3 of the electron density on each hydrogen atom to the oxygen atom (41). Huang et al. used a nonstandard form of the structure factor equation to analyze their SPC/E data:

$$S(Q) = 1 + 4\pi\rho \int_0^{R_{max}} w(r)[g(r) - 1] \frac{\sin Qr}{Qr} r^2 dr \qquad [9]$$

in which $w(r)$ is a "modification function that replaces truncation ripples in the Fourier Transform with a single unphysical bell-shaped bump at small Q the width of which is inversely proportional to the maximum distance used in $g(r)$" (16). Although the remaining oscillations in Fig. 1B of ref. 16 are attributed by Huang et al. to "poor statistics," the curves are consistent with Fourier ripples and not random noise expected from lack of convergence. In this work, the RDFs were calculated in the NVT ensemble so that Eq. 8 is defined over the small-Q region of $0.13 < Q \leq 1.0 \ \text{Å}^{-1}$, as well as in the grand canonical ensemble by sampling over spherical subvolumes of the NVT simulation so that Eq. 8 is valid over $0.14 < Q \leq 1.0 \ \text{Å}^{-1}$. The latter ensemble naturally dampens Fourier ripples as seen in Fig. 2.

To evaluate the density distributions, we randomly sample 500 cubic boxes of different lengths per configuration over 5,000 configurations, counting oxygen centers within the box, and binning the corresponding density. The density probability is calculated from the number of binned densities at a given density normalized by the number of samples.

In order to determine the anomalous component of scattering, we considered the following two models to estimate the normal component: (1) $S^N(Q)$ defined as the extrapolation of $S(Q)$ over the range $0.74 \ \text{Å}^{-1} \leq Q \leq 0.78 \ \text{Å}^{-1}$ under the constraint of reaching the $S^N(0)$ limit as was done in ref. 16, or (2) $S^N(Q) = S^N(0)$ over the entire small-Q region measured (21, 27). The values of $S^N(0)$ used in the Lorentzian function fitting procedure for experiment were calculated using Eq. 3 with values of the normal component of the isothermal compressibility χ_T^N reported by Conde et al. (42). For simulation, we calculated $S^N(0)$ from the experimental normal component of the adiabatic compressibility with the remaining thermodynamic quantities taken from the TIP4P-Ew model based on the relation provided in ref. 42.

1. Speedy RJ, Angell CA (1976) Isothermal compressibility of supercooled water and evidence for a thermodynamic singularity at −45 C. *J Chem Phys* 65:851–858.
2. Mishima O, Stanley HE (1998) Decompression-induced melting of ice IV and the liquid-liquid transition in water. *Nature* 392:164–168.
3. Starr FW, Bellissent-Funel MC, Stanley HE (1999) Structure of supercooled and glassy water under pressure. *Phys Rev E* 60:1084–1087.
4. Debenedetti PG (2003) Supercooled and glassy water. *J Phys-Condens Mat* 15:R1669–R1726.
5. Poole PH, Sciortino F, Essmann U, Stanley HE (1992) Phase-behavior of metastable water. *Nature* 360:324–328.
6. Liu Y, Panagiotopoulos AZ, Debenedetti PG (2009) Low-temperature fluid-phase behavior of ST2 water. *J Chem Phys* 131:104508.
7. Sastry S, Debenedetti PG, Sciortino F, Stanley HE (1996) Singularity-free interpretation of the thermodynamics of supercooled water. *Phys Rev E* 53:6144–6154.
8. Stillinger FH (1980) Water revisited. *Science* 209:451–457.
9. Guillot B (2002) A reappraisal of what we have learnt during three decades of computer simulations on water. *J Mol Liq* 101:219–260.
10. Clark GNI, Cappa CD, Smith JD, Saykally RJ, Head-Gordon T (2010) The structure of ambient water. *Mol Phys*, in press.
11. Hura G, Sorenson JM, Glaeser RM, Head-Gordon T (2000) A high-quality X-ray scattering experiment on liquid water at ambient conditions. *J Chem Phys* 113:9140–9148.
12. Sorenson JM, Hura G, Glaeser RM, Head-Gordon T (2000) What can X-ray scattering tell us about the radial distribution functions of water? *J Chem Phys* 113:9149–9161.
13. Soper AK (2000) The radial distribution functions of water and ice from 220–673 K and at pressures up to 400 MPa. *Chem Phys* 258:121–137.
14. Errington JR, Debenedetti PG (2001) Relationship between structural order and the anomalies of liquid water. *Nature* 409:318–321.
15. Head-Gordon T, Rick SW (2007) Consequences of chain networks on thermodynamic, dielectric, and structural properties for liquid water. *Phys Chem Chem Phys* 9:83–91.
16. Huang C, et al. (2009) The inhomogeneous structure of water at ambient conditions. *Proc Natl Acad Sci USA* 106:15214–15218.
17. Berendsen HJC, Grigera JR, Straatsma TP (1987) The missing term in effective pair potentials. *J Phys Chem* 91:6269–6271.
18. Wernet P, et al. (2004) The structure of the first coordination shell in liquid water. *Science* 304:995–999.
19. Horn HW, et al. (2004) Development of an improved four-site water model for biomolecular simulations: TIP4P-Ew. *J Chem Phys* 120:9665–9678.
20. Soper AK, Teixeira J, Head-Gordon T (2010) Is ambient water inhomogeneous on the nanometer length scale? *Proc Natl Acad Sci USA* published online: www.pnas.org/content/107/12/E44.
21. Bosio L, Teixeira J, Stanley HE (1981) Enhanced density-fluctuations in supercooled H_2O, D_2O, and ethanol-water solutions—evidence from small-angle X-ray-scattering. *Phys Rev Lett* 46:597–600.
22. Guinier A (1963) *X-ray diffraction in crystals, imperfect crystals, and amorphous bodies* (Dover Publications, Inc, New York).
23. Kell GS, Whalley E (1965) PVT properties of water. 1. Liquid water in temperature range 0 C–150 C and at pressures up to 1 Kb. *Philos Trans R Soc A* 258:565–614.
24. Moore EB, Molinero V (2009) Growing correlation length in supercooled water. *J Chem Phys* 130:244505.
25. Weeks JD, Chandler D, Andersen HC (1971) Role of repulsive forces in determining equilibrium structure of simple liquids. *J Chem Phys* 54:5237–5247.
26. Stanley HE (1971) *Introduction to phase transitions and critical phenomena* (Oxford University Press, Oxford).
27. Xie YL, Ludwig KF, Morales G, Hare DE, Sorensen CM (1993) Noncritical behavior of density-fluctuations in supercooled water. *Phys Rev Lett* 71:2050–2053.
28. Bosio L, Teixeira J, Bellissentfunel MC (1989) Enhanced density-fluctuations in water analyzed by neutron-scattering. *Phys Rev A* 39:6612–6613.
29. Hendrick RW, Mardon PG, Shaffer LB (1974) X-ray zero-angle scattering cross-section of water. *J Chem Phys* 61:319–322.
30. Michielsen JCF, Bot A, Vanderelsken J (1988) Small-angle X-ray-scattering from supercooled water. *Phys Rev A* 38:6439–6441.
31. Dings J, Michielsen JCF, Vanderelsken J (1992) Equilibrium and nonequilibrium contributions to X-ray-scattering from supercooled water. *Phys Rev A* 45:5731–5733.
32. Bellissentfunel MC, Teixeira J (1991) Dynamics of water studied by coherent and incoherent inelastic neutron-scattering. *J Mol Struct* 250:213–230.
33. Roberts CJ, Panagiotopoulos AZ, Debenedetti PG (1996) Liquid-liquid immiscibility in pure fluids: polyamorphism in simulations of a network-forming fluid. *Phys Rev Lett* 77:4386–4389.
34. Rahman A, Stillinger FH (1971) Molecular dynamics study of liquid water. *J Chem Phys* 55:3336–3359.
35. Starr FW, Harrington S, Sciortino F, Stanley HE (1999) Slow dynamics of water under pressure. *Phys Rev Lett* 82:3629–3632.
36. Pi HL, et al. (2009) Anomalies in water as obtained from computer simulations of the TIP4P/2005 model: density maxima, and density, isothermal compressibility and heat capacity minima. *Mol Phys* 107:365–374.
37. Paschek D, Ruppert A, Geiger A (2008) Thermodynamic and structural characterization of the transformation from a metastable low-density to a very high-density form of supercooled TIP4P-Ew model water. *Chemphyschem* 9:2737–2741.
38. Hura GL, et al. (2009) Robust, high-throughput solution structural analyses by small angle X-ray scattering (SAXS). *Nat Methods* 6:606–U683.
39. Wang JH, Tripathi AN, Smith VH (1994) Chemical-binding and electron correlation-effects in X-ray and high-energy electron-scattering. *J Chem Phys* 101:4842–4854.
40. Martinez L, Andrade R, Birgin EG, Martinez JM (2009) Software news and update PACKMOL: a package for building initial configurations for molecular dynamics simulations. *Journal of Computational Chemistry* 30:2157–2164.
41. Head-Gordon T, Hura G (2002) Water structure from scattering experiments and simulation. *Chem Rev* 102:2651–2669.
42. Conde O, Teixeira J, Papon P (1982) Analysis of sound-velocity in supercooled H_2O, D_2O, and water ethanol mixtures. *J Chem Phys* 76:3747–3753.

CHEMISTRY